Citation: ZHONG Linchun, YANG Yongqin, SU Ting, et al. Hybrid FDTD-PE method for predicting path loss in ship-borne communication over rough sea surfaces[J]. Natural Science of Hainan University, DOI: 10.65658/j.hndk.2025041001.

引用格式: 钟林春, 杨永钦, 苏婷, 等. 粗糙海面上预测舰载通信路径损耗的混合 FDTD-PE 方法 [J]. 海南大学学报(自然科学版中英文), DOI: 10.65658/j.hndk.2025041001.

Open Access

粗糙海面上预测舰载通信路径损耗的混合 FDTD-PE 方法

钟林春[1], 杨永钦[1], 苏　婷[1], 钟福良[1], 迟　阔[1]

（1. 海南大学 信息与通信工程学院, 海南 海口 570228）

摘　要: 针对复杂海况下舰载通信系统电波传播预测难题, 采用基于时域有限差分法 (FDTD) 与抛物方程法 (PE) 的混合建模方法。通过构建 FDTD-PE 联合算法实现近远场分域建模: 在复杂发射源区域采用 FDTD 方法建立包含粗糙海面与舰船结构的耦合模型, 精确表征电磁波源区特性; 在只有粗糙海面传播区域引入 PE 算法, 有效提升大尺度空间电磁场计算效率。为验证方法有效性, 通过与传统 FDTD 和 PE 算法的对比实验, 从计算精度、运算时间及内存消耗 3 个维度进行量化评估。结果表明, 与传统 FDTD 方法相比, FDTD-PE 混合方法具有更高的计算效率和更低的内存消耗; 与 PE 方法相比, 混合 FDTD-PE 方法具有更高的精度。该混合建模策略为复杂海洋环境下的电波传播分析提供了兼顾精度与效率的解决方案。

关键词: 时域有限差分法; 抛物方程法; 混合模型; 船舶通信; 无线电波传播

中图分类号: G312　　**文献标志码:** A

DOI: 10.65658/j.hndk.2025041001　　CSTR: 32403.14.hndk.2025041001

Hybrid FDTD-PE method for predicting path loss in ship-borne communication over rough sea surfaces

ZHONG Linchun[1], YANG Yongqin[1], SU Ting[1], ZHONG Fuliang[1], CHI Kuo[1]

（1. School of Information and Communication Engineering, Hainan University, Haikou 570228, China）

Abstract: The challenge of predicting wave propagation for ship-borne communication systems in complex marine environments is addressed by employing a hybrid modeling approach that combines the Finite-Difference Time-Domain (FDTD) method with the Parabolic Equation (PE) method. A joint FDTD-PE algorithm facilitates near-field and far-field domain modeling: the FDTD method is applied in the complex source region to establish a coupled model that includes rough sea surfaces and ship structures, accurately characterizing the electromagnetic wave source. In the propagation region, where only rough sea surfaces are present, the PE algorithm is introduced to effectively enhance computational efficiency for large-scale electromagnetic field calculations. To validate the effectiveness of the method, a comparative study with traditional FDTD and PE algorithms evaluates performance on three dimensions: computational accuracy, runtime, and memory consumption. Results demonstrate that the FDTD-PE hybrid method exhibits higher computational efficiency and lower memory consumption compared to traditional FDTD methods. methodAdditionally, the hybrid FDTD-PE method shows greater accuracy in comparison to the PE method.

Received: 2025−04−10; **Revised:** 2025−05−29; **Accepted:** 2025−06−20;

This hybrid modeling strategy provides a solution that balances precision and efficiency for electromagnetic wave propagation analysis in complex ocean environments.

Keywords: FDTD; PE; hybrid model; ship-borne communication; radio wave propagation

0 Introduction

The rapid advancement of wireless communication technologies[1] has made ship-borne communication systems[2] crucial in modern maritime operations and logistics. However, effective radio wave propagation over rough sea surfaces[3−4] remains a significant challenge. Traditional communication networks in offshore regions have limitations that require more flexible and adaptive solutions for ship-borne communication systems. Specifically, insufficient coverage from terrestrial base stations, along with the high costs[5] and bandwidth limitations[6] of satellite communications, adversely affects the reliability and efficiency of ship-borne communications.

The propagation of electromagnetic waves in marine environments is influenced by multiple factors. These include seawater conductivity, salinity, temperature, and dynamic variations of ocean waves[7]. Such factors result in significant signal attenuation[8], multipath effects[9], and phase variations[10]. These phenomena make it difficult to accurately predict wave propagation characteristics. Traditional modeling techniques have been widely used to simulate electromagnetic wave propagation. Common methods include the FDTD method[11−14], the method of moments (MOM)[15−16], the finite element method (FEM)[17], ray tracing[18], and the PE method[19−20]. The FDTD method is known for its high accuracy in simulating near-field wave behavior and complex media. However, its computational complexity grows exponentially with propagation distance, making it unsuitable for long-range modeling. In contrast, the PE method is computationally efficient for long-distance propagation in homogeneous or weakly inhomogeneous environments. However, the precision and accuracy of this method are often limited in complex marine scenarios.

To address these limitations, a hybrid method is essential for modeling the diverse propagation characteristics in marine environments. This method combines the high precision of FDTD method with the computational efficiency of PE method[21−22]. In ship-borne communications, the propagation characteristics of electromagnetic waves differ significantly between near-field and far-field regions. In the near-field region, wave behavior is primarily influenced by the signal source and medium properties. This requires high-precision modeling techniques. In the far-field region, propagation becomes more uniform. There are smaller variations in amplitude and phase, enabling efficient computation with appropriate approximations while maintaining accuracy.

This paper proposes a hybrid FDTD-PE evaluation method for analyzing path loss in ship-borne communications over rough sea surfaces. The proposed method integrates the strengths of FDTD method in near-field precision modeling and PE method in far-field efficient computation. This integration overcomes the limitations of individual approaches. It provides an accurate and efficient simulation framework for path loss in complex marine conditions. The proposed method offers a theoretical foundation for optimizing ship-borne communication systems and advances research on electromagnetic wave propagation in rough sea environments.

1 Hybrid FDTD-PE Model And Implementation

The architecture of the proposed method is schematically illustrated in Fig. 1. The computational framework consists of three principal phases. First, a two-dimensional (2D) rough sea surface is generated using the Pierson-Moskowitz (PM) spectrum[23]. This is followed by domain decomposition into near-field and far-field regions. The partitioning between the near field and the far field is based on the distance from the source of electromagnetic waves. The near field typically encompasses regions where the wavefronts are not fully developed and the effects of the source dominate, while the far field is characterized by well-defined wavefronts and decreased influence from the source. This division allows for the appropriate application of different numerical methods: the FDTD method is more suitable for the complex interactions in the near field, while the PE method efficiently handles wave propagation in the far field. The near-field region employs the FDTD method to establish the rough sea surface-ship coupling model. The PE method governs the electromagnetic propagation in the far-field region. The electromagnetic waves are excited by a ship-borne cosine-modulated Gaussian pulse source within the FDTD region. Based on the given model, the electromagnetic waves first compute near-field interactions within the FDTD computational domain. After appropriate selection of the range position, the time-domain near-field solution is transformed into a frequency-domain field distribution using the Discrete Fourier Transform (DFT). This frequency-domain distribution is then processed through strict field matching. It serves as the initial excitation for the PE algorithm. Finally, the Finite-Difference (FD) method based on the PE method is employed to model the long-range propagation of electromagnetic waves in a non-uniform atmospheric waveguide environment.

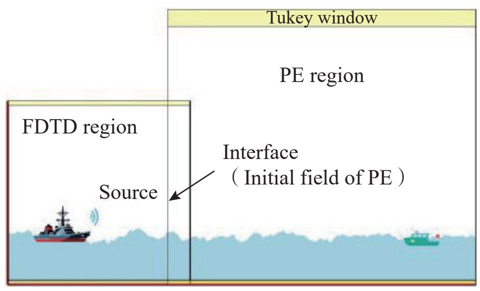

Fig. 1 Hybrid FDTD-PE ship-borne communication model.

1.1 Rough sea surface The simulation of ocean waves is a complex dynamic stochastic process. This process is typically described using spectral functions. Common spectral functions include the PM spectrum, JONSWAP spectrum, and Fung spectrum. The rough sea surface is generated using the PM spectrum, as it accurately represents the energy distribution and spectral shape of fully developed seas, validated by extensive empirical data. In contrast, the JONSWAP spectrum, optimized for fetch-limited wind-sea interactions, and the Fung spectrum, focused on high-frequency wave components, introduce additional parameters that are unnecessary for the target sea states of this paper. This spectrum was derived by Pierson and Moskowitz based on empirical data. Its mathematical expression is as follows:

$$S_1(k) = \begin{cases} \dfrac{\alpha}{4|k|^3}\exp\left(-\dfrac{\beta g_c^2}{k^2 U_{19.5}^4}\right), & k \geqslant 0 \\ 0, & k < 0 \end{cases} \tag{1}$$

where $g_c = 9.81\ \mathrm{m \cdot s^{-2}}$ is the gravitational acceleration, $U_{19.5}$ is the wind speed at a height of 19.5 m above the ocean surface, k is the wave number, while $\alpha = 8.10\times10^{-3}$ and $\beta = 0.74$ are dimensionless empirical constants.

1.2 FDTD Method The FDTD method is a well-established numerical technique for solving Maxwell's equations. It is particularly effective for simulating wave propagation in complex media. The rough sea

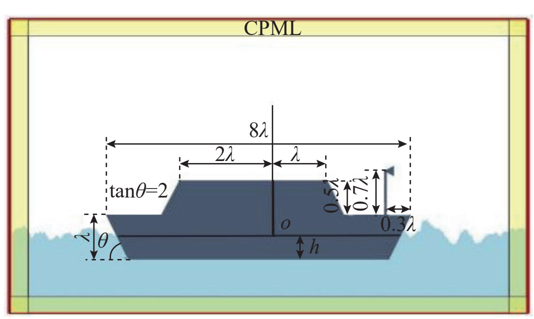

Fig. 2 Rough sea surface-ship coupling model.

surface-ship coupling model is established in the near-source region using this method. As shown in Fig. 2, the FDTD region includes the ship, the rough sea surface, and the emission source. The ship is modeled as a 2D cross-section of a small to medium-sized unmanned surface vehicle with a metallic structure. The geometric parameters are detailed in Fig. 2. Here, λ represents the wavelength at the frequency of interest, and the vessel's draft is set to $h = \lambda/2$. A Convolutional Perfectly Matched Layer (CPML) surrounds the FDTD region to absorb outgoing waves at the boundaries. This minimizes reflections and prevents non-physical artifacts.

1.3 PE Method In the *x*-*z* coordinate system, assuming a homogeneously distributed propagation medium, the field quantity ψ satisfies the 2D wave equation:

$$\frac{\partial^2\psi}{\partial x^2}+\frac{\partial^2\psi}{\partial z^2}+k^2n^2\psi=0 \tag{2}$$

where k is the wave number, and n is the refractive index. By introducing a simplified function $u(x,z)=e^{-ikx}\psi(x,z)$, (2) can be transformed into (3):

$$\frac{\partial^2 u}{\partial x^2}+2ik\frac{\partial u}{\partial x}+\frac{\partial^2 u}{\partial z^2}+k^2(n^2-1)u=0. \tag{3}$$

From (3), the forward- and backward-propagating parabolic equations can be isolated as follows:

$$\frac{\partial u}{\partial x}=-ik(1-\sqrt{Q})u, \tag{4}$$

$$\frac{\partial u}{\partial x}=-ik(1+\sqrt{Q})u, \tag{5}$$

where the pseudo-differential operator Q is defined as:

$$Q=\frac{1}{k^2}\frac{\partial^2}{\partial z^2}+n^2. \tag{6}$$

For forward propagation, the solution can be expressed as follows:

$$u(x+\Delta x,z)=e^{-ik\Delta x(1-\sqrt{Q})}u(x,z). \tag{7}$$

Starting from an initial field distribution, the field throughout the propagation domain can be solved iteratively. In this paper, the FD approach is employed to handle arbitrary boundary conditions. For the pseudo-differential operator Q, various approximation methods exist. This study adopts the Padé(1-1) approximation, which theoretically allows for an effective computation angle of up to 40°, making it suitable for wide-angle parabolic equations.

1.4 Numerical Implementation of the FDTD-PE Method The hybrid FDTD-PE method combines the FDTD and PE to simulate electromagnetic wave propagation in complex environments. The core challenge lies in seamless coupling between the FDTD and PE regions through their interface. The numerical implementation involves the following steps:

Domain Partitioning: The computational domain is divided into an FDTD region and a PE region. The FDTD region includes sources and complex terrain, bounded by CPML absorbing boundaries to minimize truncation reflections. The PE region handles simpler terrain, with a Tukey window function at the upper boundary and an impedance boundary at the lower interface.

Time-to-Frequency Domain Conversion: At the interface $x=x_{trans}$, the time-domain electric field $E(x_{trans},n\Delta t)$ from the FDTD region is converted to frequency-domain values $E(x_{trans},f)$ using the DFT:

$$E(x_{trans},f)=\Delta t\sum_{n=0}^{N}E(x_{trans},n\Delta t)\exp(-j2\pi fn\Delta t), \tag{8}$$

where N is the total number of time steps, and Δt is the time-step size. This ensures accurate initial frequency-domain fields for the PE region.

Field Transfer and Interpolation: The conjugated frequency-domain fields at the interface are transferred to the PE region. If the grid sizes between the two regions differ, spatial interpolation is applied; otherwise, direct transfer suffices. Fields within the CPML are also transferred, while non-transferred regions in PE are zero-padded.

PE Region Computation: The conjugated interface field values serve as the initial conditions for the PE region. The PE solver computes the frequency-domain field distribution across the frequencies of interest. If time-domain field recovery is required, the frequency-domain fields must be calculated for all frequency components within the signal bandwidth. Subsequently, the inverse Fourier transform is applied to reconstruct the time-domain signal from the PE results:

$$E(x,t) = \Delta f \sum_{m=-M}^{M-1} E(x, m\Delta f)\exp(j2\pi m\Delta f t), \tag{9}$$

where Δf is the frequency resolution, and M determines the signal bandwidth. The received signal incorporates the propagation delay from the interface to the receiver.

2 Numerical Results and Analysis

To validate the accuracy and effectiveness of the hybrid FDTD-PE method under the rough sea surface-ship coupling model framework, simulated results were obtained under several different wind speeds. The tests were conducted under the following conditions: (1) $U_{19.5} = 0$; (2) $U_{19.5} = 5$ m・s^{-1}; and (3) $U_{19.5} = 8$ m・s^{-1}.

In the first example, the propagation of electromagnetic waves from a ship on a calm sea surface was simulated and compared with the traditional FDTD and the PE. A propagation model, as shown in Fig. 1, was established. The model consists of two layers: the upper layer is air, and the lower layer is seawater $\varepsilon_r = 72, \sigma = 5$ s・m^{-1}, with the ship situated on the calm sea surface, and its geometric parameters are illustrated in Fig. 2. A cosine-modulated Gaussian pulse was used as the source, expressed as:

$$g(t) = E_0 \cos[2\pi f_c(t-t_0)]\exp\left[-4\pi\left(\frac{t-t_0}{\tau}\right)^2\right], \tag{10}$$

where E_0 is the pulse amplitude, and f_c is the modulation frequency. In this example, E_0=1 V・m^{-1}, $f_c = 100$ MHz, $\tau = 9.66$ ns, and $t_0 = 4.5\tau$.

In the full-region FDTD calculation, the simulation area is defined as {−150 m⩽x⩽3 600 m, −15 m⩽z⩽225 m}. The seawater region is denoted as {-150 m⩽x⩽3 600 m, -15 m⩽z⩽0 m}, while the air region is denoted as {−150 m⩽x⩽3 600 m, 0 m⩽z⩽225 m}. The grid size is $\Delta x = \Delta z$ =0.075 m, with the grid count of 50 040×3 240 and the time step of Δt =0.125 865 ns. The transmitting antenna is positioned at x = 0 m, with the source coordinates at (0, 3.6 m). Observation points are established at x_1 = (1 000 m, 3.6 m), x_2 = (2000 m, 3.6 m) and x_3 = (3 000 m, 3.6 m). In the hybrid FDTD-PE model, the transition surface is set at X_{trans} = 75 m. The FDTD simulation area is defined as {−150 m⩽x⩽75 m, −15 m⩽z⩽225 m}, with the same grid size of Δx=Δz=0.075 m and grid count of 3 640×3 240. The PE simulation area is defined as {75 m⩽x⩽3 600 m, −15 m⩽z⩽471 m}, with grid sizes of $\Delta x = 0.75$ m, $\Delta z = 0.075$ m and grid count of 4 700×6 480. Since the PE method only accounts for forward propagation and neglects backward propagation, the model retains only the region to the right of $x = 0$ from the FDTD method, while the left-side is omitted and internally modeled within the PE algorithm. The remaining settings are consistent with the PE portion of the hybrid FDTD-PE model.

The transient electric fields at the observation points were calculated using both the hybrid FDTD-PE method and the FDTD method, and the results are shown in Fig. 3. At the three observation points, the results obtained from the FDTD-PE method agree well with those from the FDTD method. The root mean square error

(RMSE) between the transient electric fields obtained by the hybrid FDTD-PE method at observation points x_1, x_2 and x_3 and the transient electric fields obtained by the FDTD method are 2.351 2e-6, 3.129 7e-6, and 4.599 8e-6, respectively. These low RMSE values indicate that the hybrid FDTD-PE method is highly accurate and reliable for modeling transient electric fields in this context.

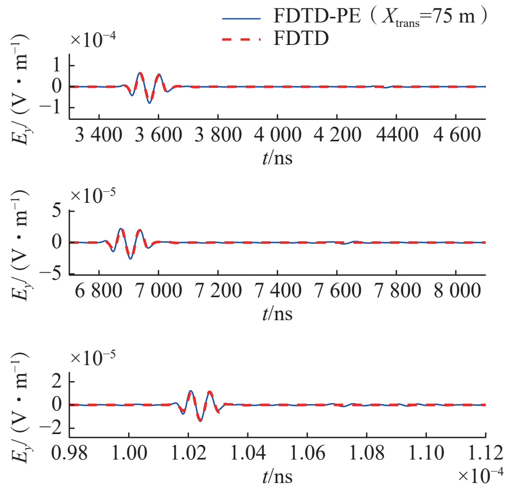

Fig. 3 Comparison of the calculated results for the transient electric field at the observation points (1 000 m, 3.6 m), (2 000 m, 3.6 m), and (3 000 m, 3.6 m).

During the numerical simulation with $U_{19.5}$ = 0, in order to further analyze the results, path losses obtained by the hybrid FDTD-PE method with transition planes set at X_{trans1} = 30 m, X_{trans2} = 75 m, and X_{trans3} =165 m were compared with those of the full FDTD method and the PE method at specific heights. The variation of path loss with distance at z = 0.9 m is shown in Fig. 4a, at z = 3.6 m in Fig. 4b, and at z = 9.0 m in Fig. 4c. At z = 0.9 m, the RMSEs between the path loss obtained by the hybrid FDTD-PE method and the FDTD method for the transition planes at X_{trans1}, X_{trans2}, and X_{trans3} are 0.820 4 dB, 0.661 4 dB, and 0.629 8 dB, respectively. In comparison, the RMSE between the path loss obtained by the PE method and the FDTD method is 3.186 0 dB. At the height of z = 3.6 m, the RMSEs for the hybrid FDTD-PE method with the three transition planes are 0.739 7 dB, 0.580 1 dB, and 0.490 2 dB, respectively, while the RMSE between the PE method and the FDTD method is 3.342 3 dB. At the height of z = 9 m, the RMSE values for the hybrid FDTD-PE method compared to the FDTD method are 0.533 1 dB, 0.346 4 dB, and 0.301 2 dB, and 7.804 3 dB for the PE method compared to the FDTD method. These results demonstrate that the hybrid FDTD-PE method achieves good consistency with the full FDTD method in path loss calculations and exhibits higher accuracy compared to the PE method, confirming the effectiveness of the FDTD-PE method in simulating electromagnetic wave propagation over a calm sea surface. The computational error between the hybrid FDTD-PE method and the full FDTD method primarily stems from two sources: one part is the inherent paraxial approximation of the PE method; specifically, the Padé(1-1) approximation used in this paper, as a first-order parabolic approximation, has inherent limitations in simulating large-angle propagation or significant backscattering. The other part originates from the field matching problem at the FDTD-PE interface, specifically the error introduced when precisely converting the time-domain full wave field computed in the FDTD region into the starter field required for the PE region at the transition plane. By comparing the results for different transition plane settings, it is found that an appropriately chosen transition position enables the hybrid FDTD-PE method results to closely match those of the FDTD method, whereas setting the transition plane too close to the ship or the transmitter may lead to larger errors. Therefore, the placement of the transition plane is crucial, as it directly determines the size of the FDTD region and thus affects computational efficiency. In general, when the wave approaches a plane wave during propagation, a good balance between accuracy and efficiency can be achieved.

In the second example, the ship-sea model is constructed based on a rough sea surface generated with a wind speed of $U_{19.5}$ = 5 m · s^{-1}, while all other numerical simulation parameters remain the same as those in the $U_{19.5}$ = 0 scenario. Fig. 5 presents the comparison results of path loss between the hybrid FDTD-PE method, the full FDTD method, and the PE method at transition planes X_{trans1} = 30 m, X_{trans2} = 75 m, and X_{trans3} =165 m, as well as at different heights (z = 0.9 m, z = 3.6 m, and z = 9 m) under a wind speed of $U_{19.5}$ = 5 m · s^{-1}. At z = 0.9 m, the RMSEs between the hybrid FDTD-PE method and the FDTD method at the three transition planes are 3.317 8 dB, 2.454 9 dB, and 1.144 6 dB, respectively, while the RMSE for the PE method is 5.316 3 dB. Similarly, at z = 3.6 m, the RMSEs for the hybrid method are 1.069 7 dB, 0.987 9 dB, and 0.581 8 dB, with the PE method yielding an RMSE of 3.220 6 dB. At z = 9 m, the RMSEs for the hybrid method are 0.986 8 dB, 0.607 8 dB, and 0.425 8 dB, while the PE method yields an RMSE of 7.942 3 dB. The accuracy of the hybrid method improves with increasing height, with particularly outstanding performance at z = 9 m, where the RMSE is significantly lower than that of the PE method. This indicates that the hybrid method maintains high accuracy under complex ocean conditions and effectively adapts to changes in wind speed. Furthermore, increasing the distance of the transition plane further reduces the RMSE, enhancing accuracy and stability in the far field.

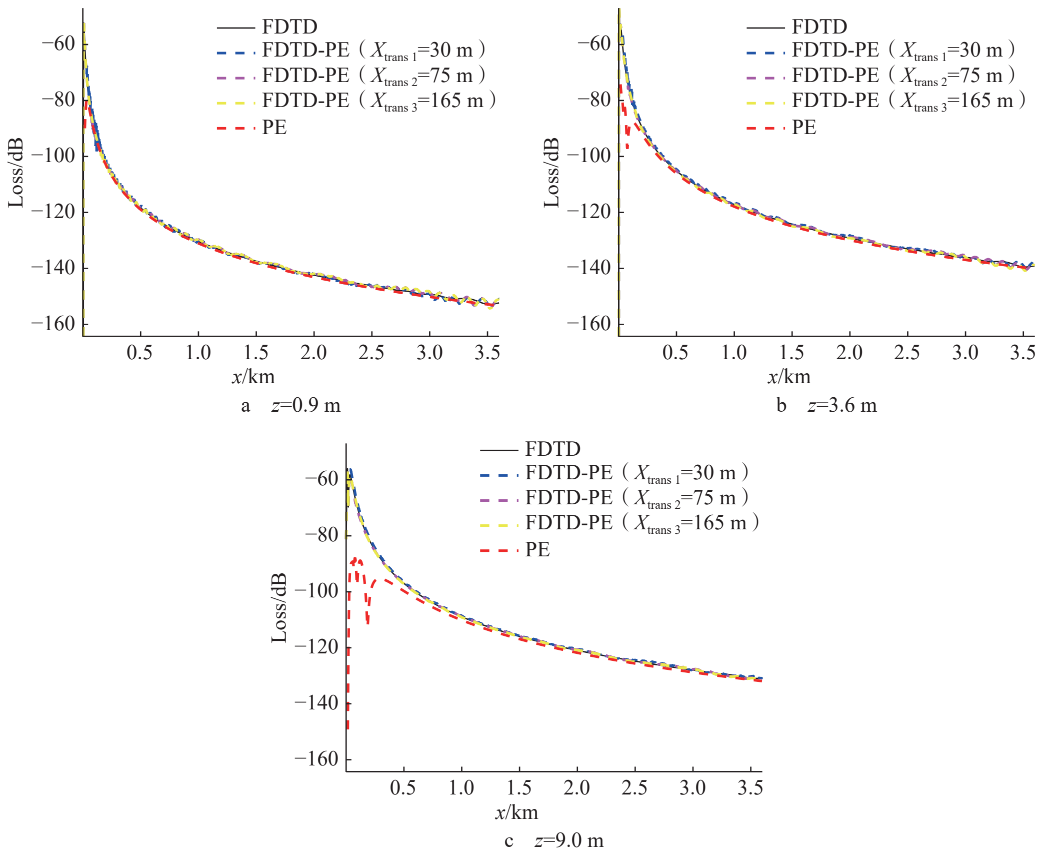

Fig. 4 Comparison of path loss obtained by different methods under $U_{19.5}$ = 0 m/s.

To further assess the applicability of the method under more challenging conditions, simulations were also conducted for $U_{19.5}$ = 8 m・s^{-1}. Fig. 6 illustrates the path loss results at different transition planes and heights. At z = 0.9 m (Fig. 6a), significant increases in path loss are observed at certain positions due to partial submersion by high waves, and the PE method—being a forward-only approximation—shows larger errors. However, at higher elevations (Figs. 6b and 6c), the hybrid method remains in good agreement with the FDTD results. At z = 3.6 m, the RMSEs for the hybrid method are 1.866 1 dB, 1.291 5 dB, and 1.000 8 dB, while the PE method yields 3.716 2 dB. At z = 9 m, the RMSEs are 1.442 7 dB, 1.138 6 dB, and 0.907 6 dB for the hybrid method, and 7.942 3 dB for the PE method. Although errors increase with wind speed and wave height, the hybrid method still outperforms the PE method in terms of accuracy.

Table 1 summarizes the average computation time and memory consumption of the FDTD, PE, and hybrid FDTD-PE methods under the three wind speed conditions. Compared to the full FDTD method, the hybrid approach achieves speedup factors of 102.06, 34.41, and 16.55 for the three transition planes, with memory savings of 78.32%, 75.68%, and 70.40%, respectively. These results indicate that the transition plane setting directly affects both computational efficiency and accuracy; more distant transition planes improve accuracy but increase resource consumption, necessitating a balanced choice. Overall, the hybrid FDTD-PE method significantly improves computational efficiency while maintaining accuracy, fully leveraging the complementary advantages of time-domain and frequency-domain solvers, and thus demonstrates strong potential for practical engineering applications.

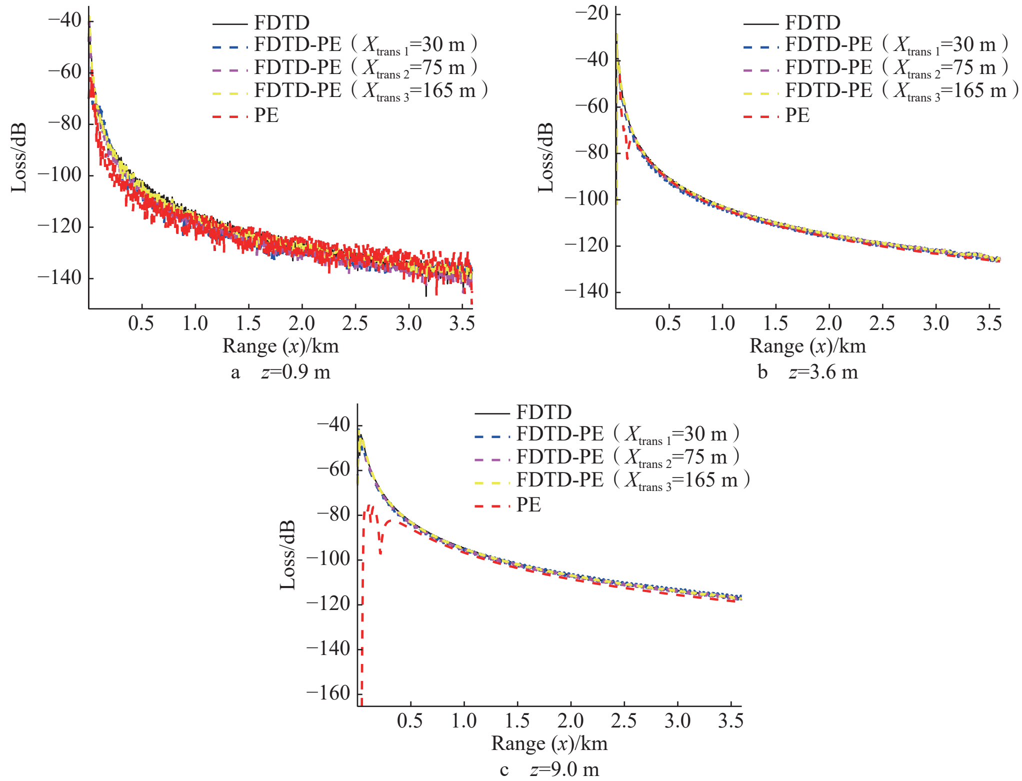

Fig. 5 Comparison of path loss obtained by different methods under $U_{19.5}$= 5 m · s^{-1}.

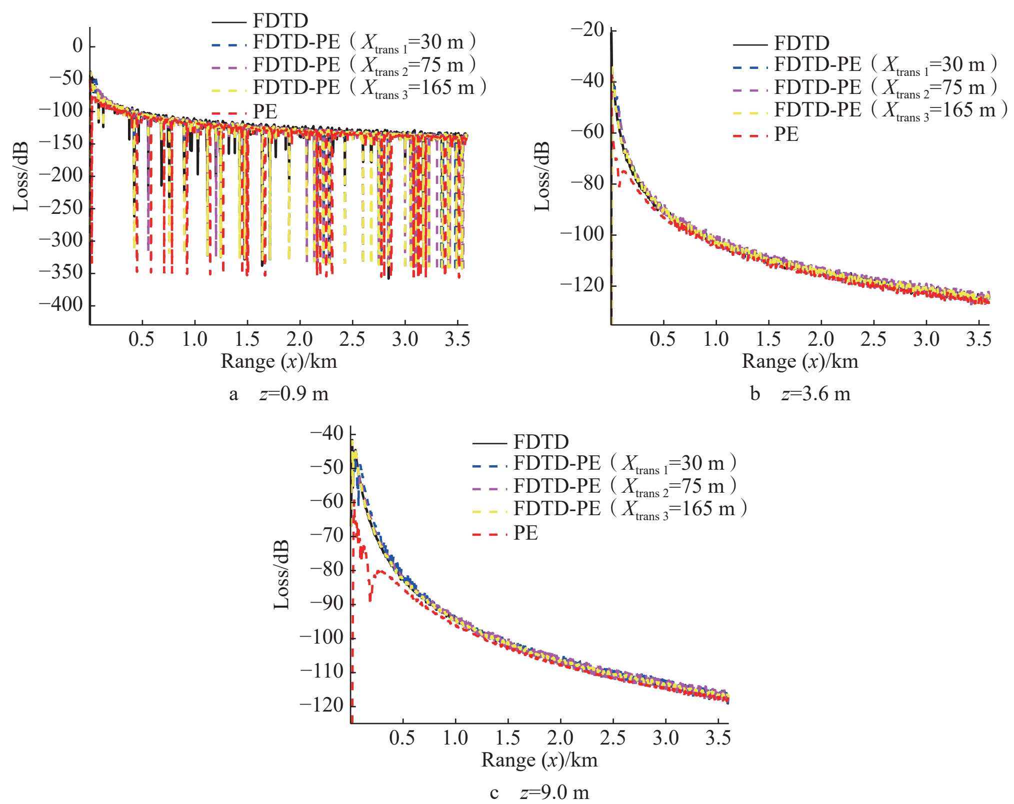

Fig. 6 Comparison of path loss obtained by different methods under $U_{19.5}$ = 8 m · s^{-1}.

Table 1 Performance comparison of FDTD-PE, FDTD, and PE methods

	FDTD-PE method			FDTD method	PE method
	X_{trans1}=30 m	X_{trans2}=75 m	X_{trans3}=165m		
Time/s	156.85	465.17	967.27	16 008.28	22.98
Memory/MB	2 931.74	3 288.52	4 002.16	13 522.74	85.12

3 Conclusion

This paper proposed and systematically evaluated a hybrid FDTD-PE method of modeling electromagnetic wave propagation in rough sea surface-ship coupling scenarios. By integrating the high accuracy of the FDTD method in the near field with the computational efficiency of the PE method for long-range propagation, the hybrid approach allows for seamless domain transition and significant resource savings. Simulation results under various wind speeds and sea conditions demonstrate that the hybrid FDTD-PE method achieves high accuracy across different heights and is especially effective in complex maritime environments, with superior performance at higher observation points compared to the conventional PE method. The study also highlights the importance of transition plane placement in balancing computational efficiency and accuracy. Overall, the hybrid FDTD-PE method proves to be a robust, efficient, and practical solution for large-scale electromagnetic propagation analysis in realistic maritime scenarios. Future work will focus on extending this framework to more diverse sea states, incorporating additional physical effects, and exploring applications in broader maritime wireless communication contexts.

References:

[1] YOU X H, WANG C X, HUANG J, et al. Towards 6G wireless communication networks: vision, enabling technologies, and new paradigm shifts[J]. Science China Information Sciences, 2021, 64(1): 110301.

[2] RONG H, CHEN M R. Influence and countermeasures on the ship-borne communication equipment of naval field complex electromagnetic environment[C]//Proceedings of 2012 11th international symposium on distributed computing and applications to business, engineering & science. Guilin: IEEE, 2012: 345−347.

[3] VORONOVICH A G, ZAVOROTNY V U. Theoretical model for scattering of radar signals in K*u* - and C-bands from a rough sea surface with breaking waves[J]. Waves in Random Media, 2001, 11(3): 247−269.

[4] YANG M Y, WU Q, ZHENG K S, et al. Analysis of propagation characteristics of low-frequency field near rough sea surface[C]//Proceedings of 2024 IEEE international conference on computational electromagnetics. Nanjing: IEEE, 2024: 1−4.

[5] WEI T, FENG W, CHEN Y F, et al. Hybrid satellite-terrestrial communication networks for the maritime internet of things: key technologies, opportunities, and challenges[J]. IEEE Internet of Things Journal, 2021, 8(11): 8910−8934.

[6] LOPES M J, TEIXEIRA F, MAMEDE J B, et al. Wi-Fi broadband maritime communications using 5.8 GHz band[C]//Proceedings of 2014 underwater communications and networking (UComms). Sestri Levante: IEEE, 2015: 1−5.

[7] LAVRENOV I V. Wind-Waves in Oceans: Dynamics and Numerical Simulations[M]. Berlin, Heidelberg: Springer, 2003.

[8] PAULL L, SAEEDI S, SETO M, et al. AUV navigation and localization: a review[J]. IEEE Journal of Oceanic Engineering, 2014, 39(1): 131−149,

[9] KARASAWA Y, SHIOKAWA T. Characteristics of L-band multipath fading due to sea surface reflection[J]. IEEE Transactions on Antennas and Propagation, 1984, 32(6): 618−623,

[10] JOHNSON J T, BURKHOLDER R J, TOPORKOV J V, et al. A numerical study of the retrieval of sea surface height profiles from low grazing angle radar data[J]. IEEE Transactions on Geoscience and Remote Sensing, 2009, 47(6): 1641−1650,

[11] YEE K S. Numerical solution of initial boundary value problems involving Maxwell's equations in isotropic media[J]. IEEE

Transactions on Antennas and Propagation, 1966, 14(3): 302−307.

[12] RODEN J A, GEDNEY S D. Convolution PML（CPML）: an efficient FDTD implementation of the CFS-PML for arbitrary media[J]. Microwave and Optical Technology Letters, 2000, 27(5): 334−339.

[13] TAFLOVE A, HAGNESS S C, PIKET-MAY M. Computational electromagnetics: the finite-difference time-domain method[M]//CHEN W K. The electrical engineering handbook. Boston: Academic Press, 2005: 629−670.

[14] SEVGI L, PAKER S. FDTD based RCS calculations and antenna simulations[J]. AEU-Archiv fur Elektronik und Ubertragungstechnik, 1998, 52(2): 65−75.

[15] JOHNSON J T, SHIN R T. A method of moments model for VHF propagation[J]. IEEE Transactions on Antennas and Propagation, 1997, 45(1): 115−125,

[16] AKLEMAN F, SEVGI L. A novel MoM- and SSPE-based groundwave-propagation field-strength prediction simulator[J]. IEEE Antennas and Propagation Magazine, 2007, 49(5): 69−82.

[17] PARKER E A, CHUPRIN A D, LANGLEY R J. Finite element analysis of electromagnetic wave diffraction from buildings incorporating frequency selective walls[J]. IEE Proceedings-Microwaves, Antennas and Propagation, 1999, 146(5): 319−323.

[18] CHEN Z J, ZHANG Y H. Offshore electromagnetic spectrum distribution prediction algorithm based on ray tracing method[J]. IEEE Antennas and Wireless Propagation Letters, 2019, 18(10): 2061−2065.

[19] WU X P, LI Z H, LIANG Z X, et al. Higher order FD-Padé scheme for 3-D parabolic equation in radio-wave propagation[J]. IEEE Antennas and Wireless Propagation Letters, 2023, 22(6): 1251−1255.

[20] GUO Q, LONG Y L. Two-way parabolic equation method for radio propagation over rough sea surface[J]. IEEE Transactions on Antennas and Propagation, 2020, 68(6): 4839−4847.

[21] WANG D D, PU Y R, XI X L, et al. Hybrid FDTD–PE method for Loran-C ASF prediction with near-source complex topography[J]. IET Microwaves, Antennas & Propagation, 2020, 14(2): 171−176.

[22] EL AHDAB Z, AKLEMAN F. An efficient 3-D FDTD-PE hybrid model for radio wave propagation with near-source obstacles[J]. IEEE Transactions on Antennas and Propagation, 2019, 67(1): 346−355.

[23] THORSOS E I. Acoustic scattering from a “Pierson–Moskowitz” sea surface[J]. The Journal of the Acoustical Society of America, 1990, 88(1): 335−349.

（责任编辑：吴　慰）